Received: 8 November 2022 | Revised: 19 December 2022 | Accepted: 19 December 2022

DOI: 10.1002/pls2.10084

RESEARCH ARTICLE

SPE POLYMERS WILEY

Bio-based polyurethane-graphene composites for adhesive application

Shivam Tiwari[1] | **Sanjai Chhaunker**[2] | **Pralay Maiti**[1]

[1]School of Materials Science and Technology, Indian Institute of Technology (Banaras Hindu University) Varanasi, Varanasi, India

[2]Hoysala Vijay Enclave, Bangalore, India

Correspondence
Pralay Maiti, School of Materials Science and Technology, Indian Institute of Technology (Banaras Hindu University) Varanasi, Varanasi-221005, India.
Email: pmaiti.mst@itbhu.ac.in

Abstract

Natural oil-based polyurethanes are prepared through solvent-less and easily processable approach for adhesive applications. The polyurethane is optimized through varying the volume fractions of the precursors which was then confirmed through the different analyses to achieve the better combination for composite formation with graphene. The graphene-polyurethane composites are processed in a simple hand mixing process with different graphene loadings and the role of the addition of graphene is studied using different analyses. The addition of graphene and the interaction with the polymer is well established through structural and thermal studies. The increase in the mechanical property with the addition of graphene to adequate amount at room temperature confirms better interfacial interaction with the polymer. The maximum peel strength obtained for the PU is around 1.05 N/mm, which supports the applicability of the prepared material for adhesive-based applications.

KEYWORDS

adhesive, castor oil, composite, graphene, polyurethane

1 | INTRODUCTION

Polyurethane (PU) is one of the remarkable material which has versatile properties like outstanding flexibility, good stability, better adhesion features based on its chemical structure which makes it a polymer with wider applicability.[1,2] Polyurethane is generally prepared using condensation reaction between the polyols and polyisocyanates in the presence of catalyst and sometimes chain extenders are also added for its preparation technique.[3] The common precursors for the PU are polyisocyanates and polyols. The polyisocyanates mostly belong to synthetic origin while the polyols can be of synthetic or bio-based origin. Bio-based polyols from natural resources are being considered nowadays to shape the biocompatibility of the polymer for even wider applications.[1] The properties and applications of the PU largely depend on the chemical nature of its precursors and the stoichiometric ratios of the NCO−/–OH groups. Based on the tunability of the PU, it is used in different areas like adhesives, coatings, foams, elastomer and composites which are well elaborated by Engels et al.[4] PU-based adhesives are replacing conventional ones because of their higher performance and biocompatibility. The adhesives developed from the PU have better adhesion properties, chemical resistance, high bond strength and faster curing kinetics. Most of the PU adhesives are prepared from synthetic precursors which affect the biocompatibility and

This is an open access article under the terms of the Creative Commons Attribution License, which permits use, distribution and reproduction in any medium, provided the original work is properly cited.
© 2023 The Authors. *SPE Polymers* published by Wiley Periodicals LLC on behalf of Society of Plastics Engineers.

biodegradability of the material, as a result, renewable natural precursors are being utilized to prepare the adhesive in recent years[1]. Several natural-based oils[5,6], lignocellulosic biomass[7], carbohydrates[8], crude glycerol[1] have been used as the polyols which provide a green route to adhesive preparation. Desai et al.[9] prepared polyester polyols using the transesterification of the potato starch and natural oil showed better adhesive properties. In another study, Kong et al.[10] prepared canola oil based PU adhesive which showed better lap shear strength. The addition of fillers or nanoparticles to the polymer matrix for enhanced properties has been a trend among researchers. Carbon-based materials are often used as reinforcing agents to improve some of the properties of polymers. The state of dispersion of fillers and therefore mixing are crucial.[11,12] Graphene is one of the remarkably efficient nanomaterial having high surface area, better electrical and mechanical properties which make it one of the most used fillers for the development of polymer composites and nanocomposites[13,14].

In this work, easy processable and highly efficient castor oil-based polyurethane is prepared in presence of polyisocyanates. The variation in isocyanate ratio and the effect on the properties of the PU is being studied to achieve the optimized ratio for the preparation of PU-graphene composites. The graphene concentration is varied to demonstrate the effect of the filler addition on different properties.

2 | MATERIALS AND METHODOLOGY

2.1 | Materials

Castor oil (CO) is procured from HiMedia, India while the toluene diisocyanate (TDI) and Dibutyltin dilaurate (DBTDL) is purchased from Sigma-Aldrich, India. Dimethyl sulphoxide (DMSO) was procured from Merck, India. Graphene was supplied by Proton Power, India. All the chemicals and products were used as received.

2.2 | Sample preparation

A cheap and easy process to prepare the polymer is used mainly from the bio-based precursors. The CO and TDI is mixed in different proportions with required amount of the catalyst DBTDL. The mixture is hand mixed to get a homogenous solution which was kept at room temperature overnight to obtain the polymer films. The different compositions used for the PU formation are stated below with the designated abbreviation.

2.2.1 | Optimizations of PU

The optimizations for PU from CO and TDI were made by varying the volume ratios of the precursors. Three samples were prepared at different volume ratios of CO:TDI and the ratios used for preparing PU were 5:1 (PU1), 2.6:1 (PU2), and 1.75:1 (PU3).

2.2.2 | PU-graphene composite preparation

Using the optimized composition of PU, different composites were prepared at different graphene compositions (2, 5, and 10 wt% with respect to polymer weight). The graphene provided was of high purity (99.9% carbon) and is multilayered. The adequate amount of the CO is taken and the required amount of graphene is added to the oil and mixed properly and then the required amount of TDI and few drops of DBTDL is added and then mixed well. Prepared PU-graphene mixture is then allowed to dry at room temperature overnight. The cross-linked composite at varying graphene compositions are denoted as PU+Gr X% (X = 2, 5, and 10) where PU denotes the optimized variations for polyurethane preparation (PU2).

2.3 | Methodology

The electronic transition of the films prepared was analyzed using the UV–visible spectrometry (JASCO V 650) in the spectral range of 200–800 nm. Fourier-transform infrared spectroscopy (FTIR) study was carried out using Thermo Scientific Nicolet Summit instrument with diamond crystal. The resolution and number of scans were 4 and 100 cm^{-1}, respectively, and the measurement was carried out in the range of 600–4000 cm^{-1}. The structural alteration in the samples were analyzed using the x-ray diffraction (XRD) measured at room temperature with copper Kα radiation. The operating conditions for Rigaku Miniflex 600X-ray diffractometer were 15 mA current and 40 kV voltages. The scan rate was fixed at 3°/min. The melting temperature and the heat of fusion of the prepared samples were analyzed using the differential scanning calorimetry (DSC) Mettler Toledo. The DSC was calibrated using the Zn/In and the sample measurement was carried out in platinum pans under nitrogen atmosphere in the temperature range − 50° to 325 °C at the rate of 10°/min. The thermal degradation behavior of the prepared samples are analyzed using the thermogravimetric analyser (TGA), Mettler Toledo from 40° to 600°C at the heating rate of 20°/min in the presence of nitrogen atmosphere.

26903857, 2023, 2, Downloaded from https://4spepublications.onlinelibrary.wiley.com/doi/10.1002/pls2.10084 by Indian Institute Of Technology, Wiley Online Library on [28/02/2024]. See the Terms and Conditions (https://onlinelibrary.wiley.com/terms-and-conditions) on Wiley Online Library for rules of use; OA articles are governed by the applicable Creative Commons License

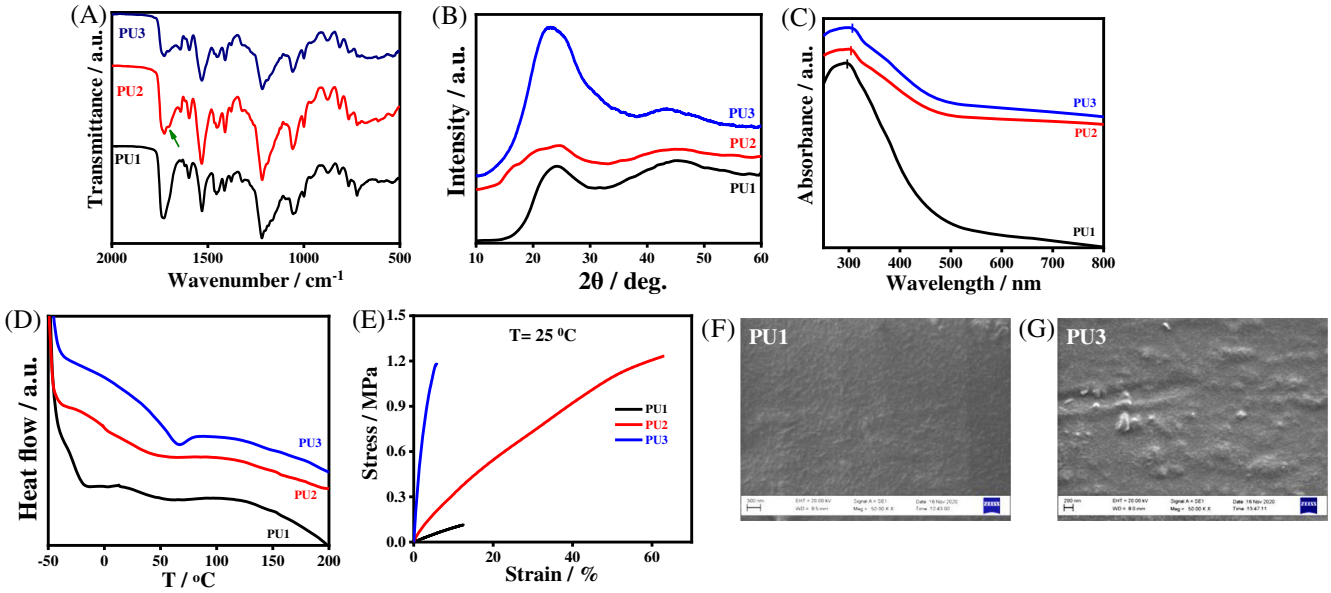

FIGURE 1 (A)) FTIR spectra; (B) XRD curve; (C) UV–vis spectra; (D) DSC thermograms; (E) stress–strain curves of the prepared polyurethanes with varying precursor ratio. SEM morphology of (F) PU1; and (G) PU3.

The mechanical properties of the prepared sample were analyzed using the universal testing machine (Tinius Olsen H50KL) at the rate of 5 mm/min. The modulus is calculated considering the linear part of the curve and the toughness is calculated from the area under the curve. The tensile properties of the samples were measured at specified dimensions at a strain rate of 5 mm/min. Peel strength of the prepared material is performed using the universal testing machine with the peel strength measurement setup. The materials were coated over the aluminum sheet of the dimension of the peel set up and were dried for 48 h prior to performing experiment. The 90° peel tests were performed at the rate of 5 mm/min at room temperature. The peel strength (N/mm) is calculated by dividing the load (N) with the width (mm) of the bonded substrates.[15] The active dimension of the aluminum substrate used for peel test was around 100 × 25 mm. The peel tests were performed for thrice for each sample and the best obtained results are presented. The morphological analyses for the films were carried out using the scanning electron microscopy (SEM) (SUPRA 40, Zeiss). The samples were gold coated before performing the characterization.

Swelling of the samples is measured using the deionized (DI) water. The samples were soaked into the respective solvent for 24 h at room temperature. After 24 h, the samples were taken out from the solvent and the solvent on the surface of the film was removed using tissue paper gently and initial and final weight of the samples before and after soaking was used to calculate the percentage (%) swelling.

$$\text{Swelling} = (W_s - W_d)/W_d,$$

where W_s and W_d are the weight of the final and initial samples, respectively.

3 | RESULTS AND DISCUSSIONS

3.1 | Optimization of polyurethane

The prepared film with the variations in the precursors (polyols and polyisocyanates) were analyzed to study the change in their characteristic features. The FTIR spectrums of the prepared PU-based films are shown in Figure 1A. The confirmatory peaks for the PU are observed at 1730, 1600, 1532, and 1221 cm^{-1} which represent the —C═O stretching, C═C bond, N—H bending, C—N stretching, respectively. The absence of the peak in the region 2250–2270 cm^{-1} which corresponds to the N═C═O group confirms that the polymerization is well established even with the simple hand mixing process[16]. A new peak arises around 1700 cm^{-1} for PU2 and PU3 which is attributed to the carbonyl group of the urethane linkage which is prominent for polyurethane with higher content of urethane linkages.[17] FTIR spectra in the range 2500–4000 cm^{-1} are shown in Figure S1 of supporting information. The N-H stretching peak for PU1, PU2, and PU3 are observed at 3338, 3310, and 3302 cm^{-1}, respectively, which arises due to the rise in the content of the hard segments due to the increase in the H-bonding

26903857, 2023, 2, Downloaded from https://4spepublications.onlinelibrary.wiley.com/doi/10.1002/pls2.10084 by Indian Institute Of Technology, Wiley Online Library on [28/02/2024]. See the Terms and Conditions (https://onlinelibrary.wiley.com/terms-and-conditions) on Wiley Online Library for rules of use; OA articles are governed by the applicable Creative Commons License

ability of polymer with higher urethane moieties. Hence, from the FTIR curve, the development of the PU is confirmed with the presence of the characteristic peaks which is well stated in the previous literature studies[18,19].

Figure 1B represents the XRD patterns of the prepared polymer. The characteristic peak for the polyurethanes is seen at 23.9° (200) which arises due to the short range periodically ordered structure of the domains of the amorphous phase of the PU[16]. Not much shifting of the peak is observed with the variation in concentration but the increase in urethane linkages concentration leads to attenuation of the peak to higher intensity which can be due to the rise in the crystalline nature of the material with increase in hard segments.[20] Figure 1C shows the UV–vis curves for the PU with the variation in precursor ratio. The absorbance peaks for the PU1, PU2 and PU3 are observed at 299, 303, and 306 nm, respectively. The increment in the wavelength may be due to increase in the urethane linkages concentration which results in the shift of π– π* transition peak and also the visible light absorption rises with increase in the urethane group content.

The thermal behavior of the prepared samples was analyzed using the differential scanning calorimetry as shown in Figure 1D. The corresponding glass transition temperature (T_g) for the prepared polyurethanes of PU1, PU2 and PU3 are around 61.1, 64.2, and 67.2 °C, respectively.[21] From the DSC curve and the respective temperature, it is clear that on increasing the content of the urethane linkages, the glass transition temperature increases due to the increment in the hard segment. The room temperature tensile test for the PU at varying polyols/polyisocyanates ratio is shown in Figure 1E. The tensile strength value for PU1, PU2, and PU3 is around 0.11, 1.24, and 1.2 MPa, respectively, while the elongation at break values for the respective samples are 12.5%, 63%, and 6%. Hablot et al.[22] prepared PU using different precursors and found the overall better mechanical properties for TDI-based system. The better mechanical property provides the required optimization for the varying volume ratios of the precursors during polymer preparation. Figure 1F, G shows the morphological image of the PU1 and PU3, respectively. The SEM micrographs clearly demonstrate that on increase in the content of the hard segments, the roughness of the surface increases due to rise in crystallinity of the polymer with increase in urethane linkages as evident from the XRD and DSC results.

The prepared samples were then subjected to deionized water (DI) to study the swelling property of the polymer. As seen from the Table ST1 in the supporting information, that the percentage swelling increases with the increment in the urethane linkages which can be due to the higher content of the polar groups favoring the swelling of the polymer film. The better mechanical property provides the required optimization for the varying volume ratios of the precursors during polymer preparation.

3.2 | Analysis of polyurethane-graphene composites properties

The change in the electronic transition is observed through the UV–vis analysis for the graphene-optimized PU composite as shown in Figure 2A. The absorbance peak for PU, PU+Gr2, PU+Gr5, and PU+Gr10 is seen around 303, 301, 299, and 294 nm, respectively. The increment in the graphene concentration leads to blue shift which can be attributed to the smaller dimension of the graphene which provides constraint environment in the polymer and increases the absorbance with graphene loading. The UV–vis curve for the graphene is shown in Figure S2 of supporting information shows the broad peak. The absorbance curve gets broaden at higher wavelength region on graphene addition which confirms

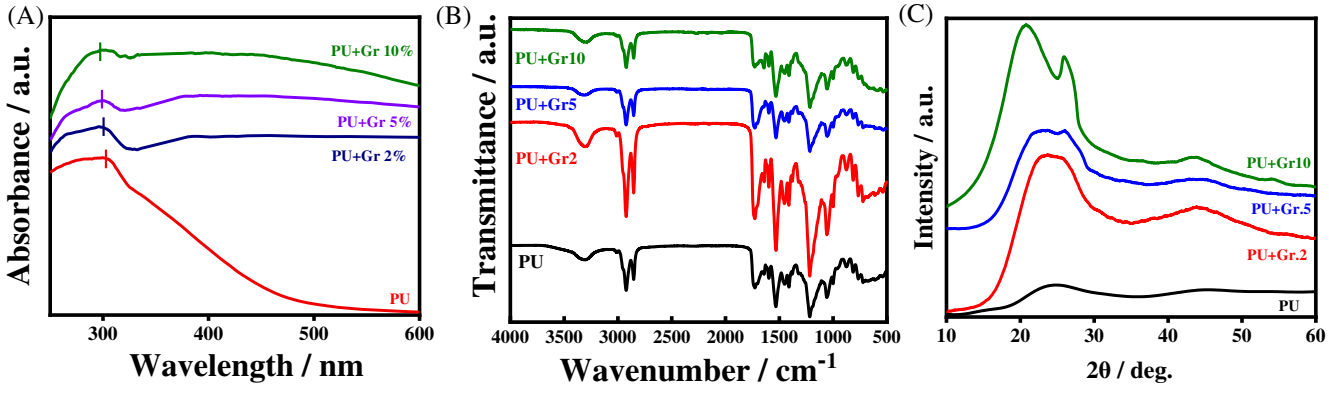

FIGURE 2 (A)) UV–vis plot; (B) FTIR spectra; and (C) XRD curves for the pristine optimized polyurethane and its graphene-based composites at different graphene loading.

26903857, 2023, 2, Downloaded from https://4spepublications.onlinelibrary.wiley.com/doi/10.1002/pls2.10084 by Indian Institute Of Technology, Wiley Online Library on [28/02/2024]. See the Terms and Conditions (https://onlinelibrary.wiley.com/terms-and-conditions) on Wiley Online Library for rules of use; OA articles are governed by the applicable Creative Commons License

better interaction of the graphene with the PU. The FTIR peaks for the pure PU and the graphene-based composite films at different graphene loadings are shown in Figure 2B. The characteristic peak for the N—H stretching is seen around 3310 cm^{-1}which shifts to 3300 cm^{-1}on graphene loading. The carbonyl stretching peak is found to be at 1730 cm^{-1}. The FTIR spectra peak for C═C, C—N stretching and C—O bonds is seen around 1601, 1532, and 1055 cm^{-1}, respectively. The peaks after the addition of the graphene do not show any prominent shift but some attenuation in the intensity values. The absence of any shifting in FTIR bands suggests that the graphene addition to the PU matrix does not alter any of the functional groups of the polymer. Similar observation was also reported in the previous literature studies.[23] The effect of graphene addition to the PU matrix is analyzed using the XRD as revealed in Figure 2C. The characteristic peak for the PU is at 24° (200) while the graphene shows the major crystalline peak at 26.4° (002) (Figure S3). The prepared graphene-PU composite shows two peak at 23.2° and 26° (for PU+Gr5), which the confirmatory peaks for the PU and graphene with some shifting due to the composite formation. The XRD peak of PU +Gr10 is observed at 21° which has considerably shifted after graphene loading. The increase in the addition of the graphene content result in sharp increase in the graphene peak which further confirms the better interfacial interaction of the polymer-nanoparticle in the composite prepared using simple process.

The morphological investigation is carried out using the scanning electron microscopy as shown in Figure 3. The pristine PU (Figure 3 A) showed a uniform morphology with no such roughness while on varying the precursor ratio for the PU preparation, the morphology varies. The addition of graphene leads to change in morphology with a rough surface as seen in Figure 3 B. Addition of higher content of graphene (Figure 3 C) leads to agglomeration which is clearly visible from the SEM image of the PU+Gr 10. Hence, the addition of graphene to certain concentration produces some significant changes in the morphology of the composite film which gets completely altered on increase in the graphene content.[23] The thermal behavior of the prepared films against temperature is shown in Figure 4. The differential scanning calorimetry curves for the neat PU and the prepared composite films are presented in Figure 4 A. The

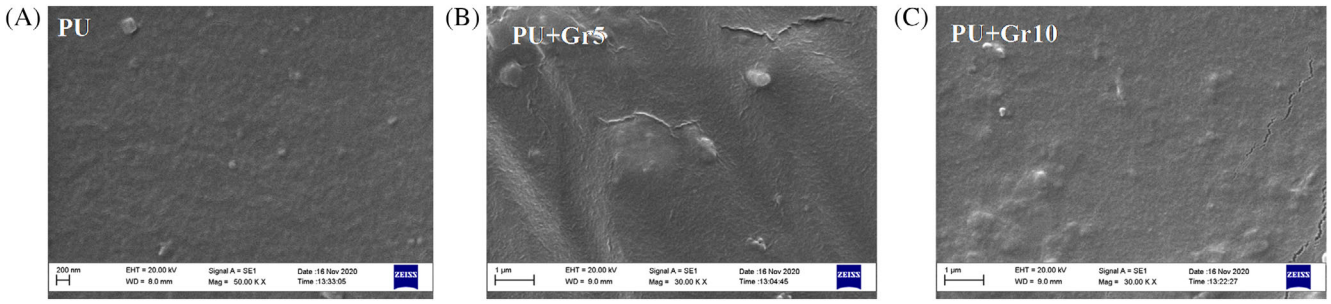

FIGURE 3 SEM surface morphologies of (A) PU; (B) PU+Gr5, and (C) PU+Gr10

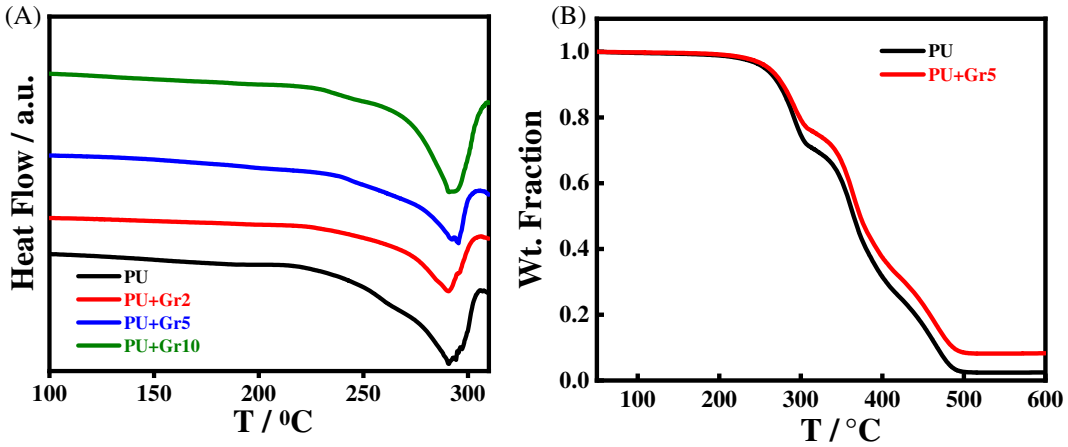

FIGURE 4 (A) DSC thermograms of the neat optimized polyurethane and its composite with grapheme; and (B) TGA plot of the prepared PU and its graphene-based composite at different graphene loadings.

26903857, 2023, 2, Downloaded from https://4spepublications.onlinelibrary.wiley.com/doi/10.1002/pls2.10084 by Indian Institute Of Technology, Wiley Online Library on [28/02/2024]. See the Terms and Conditions (https://onlinelibrary.wiley.com/terms-and-conditions) on Wiley Online Library for rules of use; OA articles are governed by the applicable Creative Commons License

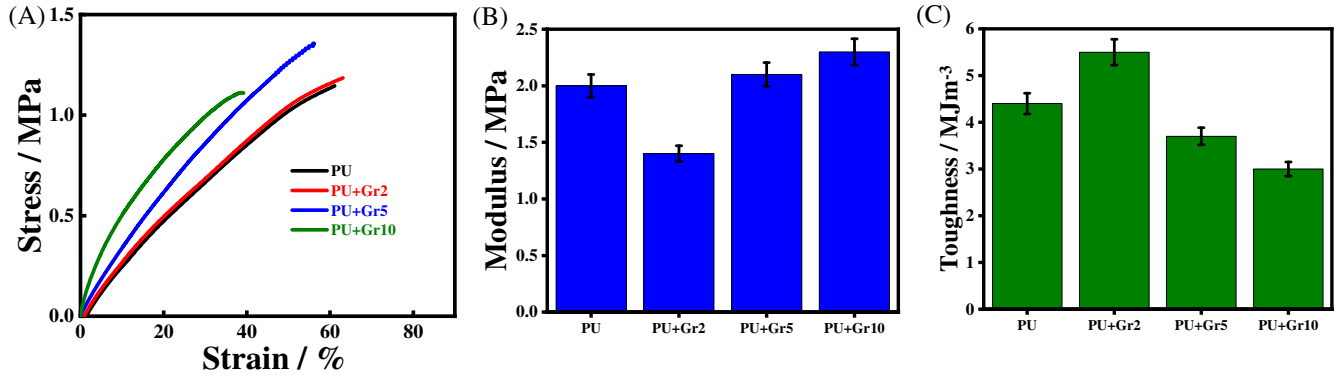

FIGURE 5 (A) Stress–strain curves of the PU and its composite films; calculated (B) modulus; and (C) toughness of the films from area under the stress–strain curves.

melting peak for the PU is around 289.5°C which increases to 292.1°C for PU+Gr 5. Addition of graphene to the PU does vary the melting temperature of the composite which can be associated with the change in the crystal segments of the polymer matrix on graphene loading. Figure 4 B shows the TGA curves of the PU and its composite in the presence of nitrogen atmosphere. The major degradation peak for the PU is observed around 250–290°C and 350–400°C which on addition of the graphene nanoparticles increases to higher temperature. The representative DTG curve is shown in Figure S4 of supporting information. The 5% degradation (weight loss) of the PU occurs at 256°C while for PU+Gr5 the degradation temperature rises to 264°C, indicating better thermal stability of the graphene based composite. The first step degradation is mainly associated to the cleavage of the urethane linkages while the second step degradation is attributed to the decomposition of the soft segments, that is, the polyols.[24] Nearly complete degradation of the material is observed beyond 450°C for PU. Similar observation has been well-stated with possible mechanism of degradation in the previous literature[22]. Addition of graphene improves the thermal stability of the composites which can be due to the high surface area of the nanomaterial that provides a path for better thermal stability with higher degradation temperature which can be visualized as almost complete degradation of the PU occurs around 500°C while the prepared composites is not completely degraded even at higher temperature. The role of graphene addition and the PU degradation behavior is in well accordance with the previous literature studies.[25,26]

The mechanical properties at room temperature (RT) and lower temperature (LT) are shown in Figure 5. The addition of graphene to the PU matrix and its effect based on temperature of operation is well explained. The stress–strain curve for the PU and its composite at RT are presented in Figure 5A. The calculated Young's modulus (Figure 5B) and the toughness values (Figure 5C) from the stress–strain curves for the PU are around 1.9 MPa and 4.4 MJm^{-3}, respectively. On graphene loading at different concentrations, the modulus and the toughness value gets altered due to the interaction with the polymer. The obtained modulus for PU+Gr2, PU+Gr5 and PU+Gr10 are around 1.4, 2.1 and 2.3 MPa, respectively, whereas the toughness value obtained for the prepared composites are nearly 5.5, 3.7, and 3.0 MJm^{-3}, respectively. From the obtained values of the modulus and toughness, it can be observed that the addition of graphene increases the modulus and there is a decrease in toughness after a particular loading of graphene. The mechanical property for the composite depends on the better dispersion and profound interfacial interaction between the polymer and the filler.[26] From the obtained values, it can be seen that at higher loading of the graphene, the mechanical property, especially the toughness deteriorates with the reduction in the elongation at break. The influence of the nanoparticle aggregation with reduction in mechanical properties is well-explained in the previous literature studies.[27,28] From the obtained values it can be observed that there has been considerable increase in mechanical properties value in the PU +Gr5 composite as compared to the pristine polymer. The better mechanical properties of graphene are well established with the polymer-based composite even at lower temperatures. The reduction in the mechanical properties at higher graphene loading is also observed as seen at RT. The mechanical integrity of the corresponding nanocomposite and its mechanical performance are strongly influenced by the interfacial interactions between polymers and graphene-based materials. The precise management of the graphene nanofillers' dispersion and distribution ensures the best possible exposure of the graphene surface to the polymer matrix and a successful reinforcement of the mechanical properties.

26903857, 2023, 2, Downloaded from https://4spepublications.onlinelibrary.wiley.com/doi/10.1002/pls2.10084 by Indian Institute Of Technology, Wiley Online Library on [28/02/2024]. See the Terms and Conditions (https://onlinelibrary.wiley.com/terms-and-conditions) on Wiley Online Library for rules of use; OA articles are governed by the applicable Creative Commons License

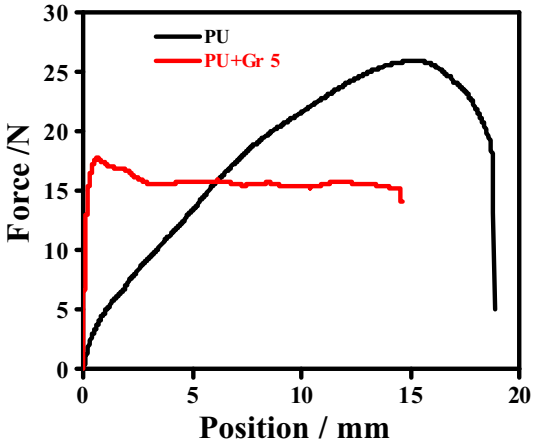

FIGURE 6 Peel test of the pristine PU and optimized composite (PU+Gr5).

Strong interfacial binding can change the shape of macromolecules close to the filler surface, despite the enormous surface to volume ratio of graphene that may lead to high binding efficiency once disseminated. The mechanical capabilities of an adhesive formulation are significantly enhanced by the inclusion of graphene in an adequate amount. The enhancement of the favorable contacts between the adhesive matrix and the distributed graphene sheets is what gives the graphene its reinforcing effect. The state of dispersion and the interfacial adhesion between graphene and a polymer matrix plays a key role to generate good mechanical and other properties, as reported in the literature.[29] On the other hand, adding higher content of graphene causes the mechanical characteristics of the composite to deteriorate because the graphene sheets begin to aggregate into the matrix and form heterogeneous domains which affects the mechanical properties.[23,30,31]

Peel strength is one of the important properties to demonstrate the practical applicability of the material. The peel test analysis is presented in Figure 6. The maximum load required to peel off the two adhered substrates are around 26.2 and 18 N for PU and PU+Gr5, respectively. The maximum load is higher in case of the pristine polymer due to the better adhesion with the substrates as compared to the composite. The maximum peel strength obtained for the PU and PU+Gr5 are around 1.05 and 0.72 N/mm, respectively.

Baudrit et al.[32] showed the effect of nanosilica addition on the adhesive property of the polyurethane. From the obtained curve of the peel test, it can be seen that the curve increases linearly with the load for PU till it reaches the maximum values after which the force reduces due to the separation of substrates. While in case of PU-graphene composite, the curve rises linearly with the applied load as seen in the PU part but the discontinuity in the peeling off of the interconnected substrates is minimal in case of graphene-based adhesives. For the PU+Gr5, it can be seen that to initiate the peeling process, very high load is needed as compared to the PU which suggests that the adhesion between the substrates requires maximum force in presence of graphene. Also almost an equivalent force is required to peel off the substrates adhered with composite-based adhesive which explains the better mixing of the graphene with the polymer and the better surface-volume ratio of the nanoparticle provides good interfacial interaction which results in uniform adhesion between the layers. While in case of the PU, higher force is achieved which can be due to the better inter-chain interaction between the precursors resulting in efficient polymerization even through the simple fabrication process which provides effective adhesion between the substrates. Hence, from the obtained peel strength values, it is suggested that both the prepared adhesives are of practical application depending on the requirement of the application.

4 | CONCLUSIONS

In this work, castor oil-based polyurethane is prepared from a simple and easily processable technique. Polyurethane is being optimized by varying the volume ratio of the precursors which was analyzed using different characterizations to point out the better combination of the precursors for composite preparation. The optimized PU composition was PU2 (CO:TDI = 2.6:1) which showed better mechanical property in comparison with the other variants and was further used for graphene-based composite preparation. Graphene is added to the optimized polyurethane to form a composite film using solvent-less and are easily processable. The addition of the graphene to the polyurethane-based adhesives provides better mechanical strength as compared to the pristine polymer. The modulus increases to around 12.5% in case of the tensile test performed at room temperature for the composite with 5% graphene loading at lower temperature tensile testing. Graphene loading provides better interfacial interaction with the polymer which results into higher mechanical properties. Also the peel test showed a uniform cleavage of the adhered substrates in case of the PU+Gr5 while maximum peel strength is obtained for the pristine PU which was around 1.05 N/mm. The addition of graphene to PU increases the interfacial adhesion which requires higher force to initiate the peeling as compared to neat PU. The prepared materials show a better mechanical and peel strength which can be an

26903857, 2023, 2, Downloaded from https://4spepublications.onlinelibrary.wiley.com/doi/10.1002/pls2.10084 by Indian Institute Of Technology, Wiley Online Library on [28/02/2024]. See the Terms and Conditions (https://onlinelibrary.wiley.com/terms-and-conditions) on Wiley Online Library for rules of use; OA articles are governed by the applicable Creative Commons License

effective material for adhesive application for different substrates.

ACKNOWLEDGMENT

The author would like to acknowledge the institute for providing the teaching assistantship and Central Instrument Facility (CIF), IIT (BHU) Varanasi for the required characterizations.

CONFLICT OF INTEREST

The authors have no conflict of interest to report.

DATA AVAILABILITY STATEMENT

Data are available on request.

ORCID

Pralay Maiti https://orcid.org/0000-0002-6879-3591

REFERENCES

[1] S. Cui, X. Luo, Y. Li, *Int. J. Adhes. Adhes.* **2017**, *79*, 67.
[2] A. Fakhar, S. Maghami, E. Sameti, M. Shekari, M. Sadeghi, *SPE Polym.* **2020**, *1*, 113.
[3] R. B. Seymour, G. B. Kauffman, *J. Chem. Educ.* **1992**, *69*, 909.
[4] H. W. Engels, H. G. Pirkl, R. Albers, R. W. Albach, J. Krause, A. Hoffmann, H. Casselmann, J. Dormish, *Angew. Chemie Int. Ed.* **2013**, *52*, 9422.
[5] M. M. Aung, Z. Yaakob, S. Kamarudin, L. C. Abdullah, *Ind. Crops Prod.* **2014**, *60*, 177.
[6] M. Malik, R. Kaur, *Adv. Polym. Technol.* **2018**, *37*, 24.
[7] R. Briones, L. Serrano, R. Ben Younes, I. Mondragon, J. Labidi, *Ind. Crops Prod.* **2011**, *34*, 1035.
[8] A. J. de Menezes, D. Pasquini, A. A. S. Curvelo, A. Gandini, *Biomacromolecules* **2007**, *8*, 2047.
[9] S. D. Desai, J. V. Patel, V. K. Sinha, *Int. J. Adhes. Adhes.* **2003**, *23*, 393.
[10] X. Kong, G. Liu, J. M. Curtis, *Int. J. Adhes. Adhes.* **2011**, *31*, 559.
[11] G. H. Hu, S. Hoppe, L. F. Feng, C. Fonteix, *Chem. Eng. Sci.* **2007**, *62*, 3528.
[12] F. You, D. Wang, J. Cao, X. Li, Z. M. Dang, G. H. Hu, *Polym. Int.* **2014**, *63*, 93.
[13] T. Kuilla, S. Bhadra, D. Yao, N. H. Kim, S. Bose, J. H. Lee, *Prog. Polym. Sci.* **2010**, *35*, 1350.
[14] S. Armin, S. Esfahani, N. Ghahramani, | M. Mehranpour, H. Nazockdast, *SPE Polym.* **2021**, *2*, 134.
[15] S. F. Dana, D. V. Nguyen, J. S. Kochhar, X. Y. Liu, L. Kang, *Soft Matter.* **2013**, *9*, 6270.
[16] S. Thakur, N. Karak, *Prog. Org. Coatings* **2013**, *76*, 157.
[17] A. Mishra, V. K. Aswal, P. Maiti, *J. Phys. Chem. B* **2010**, *114*, 5292.
[18] S. Lin, J. Huang, P. R. Chang, S. Wei, Y. Xu, Q. Zhang, *Carbohydr. Polym.* **2013**, *95*, 91.
[19] S. Gogoi, N. Karak, A. C. S. Sustain, *Chem. Eng.* **2014**, *2*, 2730.
[20] A. Mishra, B. P. Das Purkayastha, J. K. Roy, V. K. Aswal, P. Maiti, *J. Phys. Chem. C* **2012**, *116*, 2260.
[21] B. Adak, M. Joshi, B. S. Butola, *Compos. B: Eng.* **2019**, *176*, 107303.
[22] E. Hablot, D. Zheng, M. Bouquey, L. Avérous, *Macromol. Mater. Eng.* **2008**, *293*, 922.
[23] L. Cristofolini, G. Guidetti, K. Morellato, M. Gibertini, M. Calvaresi, F. Zerbetto, M. Montalti, G. Falini, *ACS Omega* **2018**, *3*, 8829.
[24] C. Miranda, J. Castaño, E. Valdebenito-Rolack, F. Sanhueza, R. Toro, H. Bello-Toledo, P. Uarac, L. Saez, *Polym.* **2020**, *12*, 1934.
[25] H. Liu, M. Dong, W. Huang, J. Gao, K. Dai, J. Guo, G. Zheng, C. Liu, C. Shen, Z. Guo, *J. Mater. Chem. C* **2017**, *5*, 73.
[26] J. Bian, H. L. Lin, F. X. He, X. W. Wei, I. T. Chang, E. Sancaktar, *Compos. Part A: Appl. Sci. Manuf.* **2013**, *47*, 72.
[27] K. Hu, D. D. Kulkarni, I. Choi, V. V. Tsukruk, *Prog. Polym. Sci.* **1934**, *2014*, 39.
[28] H. Kim, A. A. Abdala, C. W. MacOsko, *Macromolecules* **2010**, *43*, 6515.
[29] F. You, D. Wang, X. Li, M. Liu, Z. M. Dang, G. H. Hu, *J. Appl. Polym. Sci.* **2014**, *131*, 40455.
[30] M. Terrones, O. Martín, M. González, J. Pozuelo, B. Serrano, J. C. Cabanelas, S. M. Vega-Díaz, J. Baselga, O. Martín, M. González, J. Pozuelo, B. Serrano, J. C. Cabanelas, J. Baselga, M. Terrones, S. M. Vega-Díaz, *Adv. Mater.* **2011**, *23*, 5302.
[31] M. Fang, K. Wang, H. Lu, Y. Yang, S. Nutt, *J. Mater. Chem.* **2009**, *19*, 7098.
[32] J. Vega-Baudrit, V. Navarro-Bañón, P. Vázquez, J. M. Martín-Martínez, *Int. J. Adhes. Adhes.* **2006**, *26*, 378.

SUPPORTING INFORMATION

Additional supporting information can be found online in the Supporting Information section at the end of this article.

How to cite this article: S. Tiwari, S. Chhaunker, P. Maiti, *SPE Polym.* **2023**, *4*(2), 41. https://doi.org/10.1002/pls2.10084

26903857, 2023, 2, Downloaded from https://4spepublications.onlinelibrary.wiley.com/doi/10.1002/pls2.10084 by Indian Institute Of Technology, Wiley Online Library on [28/02/2024]. See the Terms and Conditions (https://onlinelibrary.wiley.com/terms-and-conditions) on Wiley Online Library for rules of use; OA articles are governed by the applicable Creative Commons License